drugs and drug candidates

MDPI

Article

Thalidomide-Based PROTACs: A Viable Strategy Against Trypanosomatids?

Romina Manarin [1], Gianfranco Frattini [1,2], Victoria L. Alonso [1,3], Victoria Boselli [1,3], Giselle R. Bedogni [1], Elvio Rodríguez Araya [1,3], Diego M. Moreno [1,2] and Esteban Serra [1,3,*]

[1] Facultad de Ciencias Bioquímicas y Farmacéuticas, Universidad Nacional de Rosario, Suipacha 531, Rosario CP 2000, Santa Fe, Argentina; romimanarin@gmail.com (R.M.); gfrattini97@gmail.com (G.F.); alonso@ibr-conicet.gov.ar (V.L.A.); boselli@ibr-conicet.gov.ar (V.B.); gisellebedogni@gmail.com (G.R.B.); rodriguezaraya@ibr-conicet.gov.ar (E.R.A.); moreno@iquir-conicet.gov.ar (D.M.M.)

[2] Instituto de Química Rosario (IQUIR), Consejo Nacional de Investigaciones Científicas y Técnicas (CONICET)-UNR, Ocampo y Esmeralda, Rosario CP 2000, Santa Fe, Argentina

[3] Instituto de Biología Molecular y Celular Rosario (IBR), Consejo Nacional de Investigaciones Científicas y Técnicas (CONICET)-UNR, Ocampo y Esmeralda, Rosario CP 2000, Santa Fe, Argentina

* Correspondence: serra@ibr-conicet.gov.ar

Abstract

Background: In recent years, compounds known as Proteolysis Targeted Chimeras (PROTACs) have revitalized the field of bioactive molecule design. These compounds promote proteolysis of therapeutic targets by recruiting them to ubiquitin ligases. One of the most commonly used classes of compounds in the synthesis of PROTACs are immunomodulatory imides (IMiDs), such as thalidomide (TLD), which interact with the E3 ligase $CRL4^{CRBN}$ via the CULT domain of the cereblon protein (CRBN). This domain has been identified in proteins across various phylogenetic groups, including trypanosomatids, leading to the hypothesis that IMiD-derived PROTACs should be active in these organisms. **Methods:** The trypanocidal activity of the PROTAC dBET1 and its separated components (JQ1 and TLD) were assayed using a *T. cruzi* strain expressing β-glalactosidase. Potential CRL4-E3L complexes from humans and trypanosomatids were assembled in silico with MultimerMapper. The IMiD-binding site of HsCRBN and its trypanosomatid homologs were analyzed using molecular dynamics and docking simulations. **Results:** We demonstrate that the compound dBET1 does not function as a PROTAC in *Trypanosoma cruzi*. In silico structural analysis of CRL4-E3L complex orthologs revealed that the trypanosomal CULT-containing protein is not part of such a complex. Molecular dynamics simulations showed that the pocket of this CULT domain is smaller than that of mammalian CRBN and cannot accommodate IMiDs within. **Conclusions:** We underscore the importance of functional and structural validation in drug discovery, particularly when extrapolating mechanisms between evolutionarily distant species. While PROTACs hold promise in human therapeutics, our work advocates for re-evaluating the rationale behind thalidomide-based PROTACs in trypanosomatid research.

Keywords: PROTAC; BET inhibitors; drug discovery; trypanocides

Academic Editor: Philippe Loiseau

Received: 27 October 2025
Revised: 26 November 2025
Accepted: 2 December 2025
Published: 10 December 2025

Citation: Manarin, R.; Frattini, G.; Alonso, V.L.; Boselli, V.; Bedogni, G.R.; Rodríguez Araya, E.; Moreno, D.M.; Serra, E. Thalidomide-Based PROTACs: A Viable Strategy Against Trypanosomatids? *Drugs Drug Candidates* **2025**, *4*, 55. https://doi.org/10.3390/ddc4040055

1. Introduction

The traditional approach to drug discovery and design relies on the ability of low-molecular-weight organic compounds to bind with high affinity to proteins that possess receptor or enzymatic activity, thereby inhibiting their function. However, many proteins

that are potential therapeutic targets lack such activities and are therefore not amenable to this conventional strategy. This limitation has been addressed by the development of PROTACs (Proteolysis Targeting Chimeras), bifunctional molecules that simultaneously bind to a protein of interest (POI) and an E3 ubiquitin ligase complex, leading to the ubiquitination and subsequent degradation of the POI by the proteasome [1,2]. Moreover, many compounds with good specificity and moderate affinity for essential proteins (regardless of whether these proteins are conventional drug targets) often show limited in vivo activity, which can be enhanced by converting them into PROTACs.

E3 ubiquitin ligases, along with E2 ubiquitin-conjugating enzymes and E1 ubiquitin-activating enzymes, form the core components of the cellular ubiquitination machinery [3]. E3 ligase complexes typically consist of three to five subunits, one of which functions as a substrate receptor. Although hundreds of such substrate receptors exist, most PROTACs developed to date utilize only a few of them, including CRBN, cIAP1, VHL, and MDM2. Among the most explored PROTACs are those that employ immunomodulatory imide drugs (IMiDs), such as thalidomide and its derivatives lenalidomide and pomalidomide, to recruit the protein target to a E3 ligase via a specific receptor named cereblon (CRBN) [4].

CRBN functions as the substrate receptor within a Cullin-RING ubiquitin ligase (CRL) complex, also known as $CRL4^{CRBN}$, which also includes the proteins DDB1, CUL4A/4B, and RBX1. In this complex CRBN is responsible for recognizing and binding target proteins for ubiquitination [5]. Although the physiological function of CRBN is not completely known, it has been associated with numerous regulatory events in cells [6]. CUL4A/B, a member of the cullin protein family, play a central scaffolding role in this complex. Its N-terminus binds to a β-propeller domain of the adaptor protein DDB1 (Damaged DNA-Binding 1), which further associates with various factors, including CRBN [5]. CUL4A also interacts, via its C-terminus, with the RING domain protein RBX1 (also known as ROC1), which facilitates the recruitment of E2 ubiquitin-conjugating enzymes. Together, the C-terminal domain of CUL4A, RBX1, and activated E2 enzymes form the catalytic core of the CRL4 complex [7].

CRBN contains two LON domains in its N-terminal region, flanked by an α-helical segment involved in binding DDB1, and a CULT domain (Cereblon domain of Unknown activity, binding cellular ligands and thalidomide) in the C-terminal region [8]. The CULT domain comprises two antiparallel β-sheets arranged at approximately a right angle and stabilized by a structural zinc ion. The protein family known as the CULT domain family is defined by the presence of this domain and has proteins found throughout eukaryotes, except fungi, and prokaryotes [8]. Based on sequence comparison and homology modeling, it has been proposed that the pocket where IMiDs binds with CRBN is conserved and, hence, that thalidomide-based PROTACs could also be used to target infectious agents that have one CULT-domain protein [9–11].

Chagas disease, caused by *Trypanosoma cruzi*, is a disease of American origin that is currently expanding geographically due to increased population migration. The number of affected individuals is estimated to be at least at 7 million, and the drugs available for its treatment have limited therapeutic activity and significant side effects [12]. In this context, PROTAC strategies represent enormous potential for the development of new trypanocides [13]. Other species of the order Trypanosomatida, including two subspecies of *Trypanosoma brucei* and the species complex of the genus *Leishmania*, responsible for sleeping sickness and different forms of leishmaniasis in humans, are also considered neglected diseases.

Members of trypanosomatids' ubiquitin-mediated protein degradation system have been computationally identified through genome analyses but remain only partially char-

acterized at the experimental level [9,14–19]. Considered themselves as potential drug targets by their own right, trypanosomatids have homologs of the E1, E2, and E3 enzyme families, though in a lower quantity than humans. Among these, it was identified that a CULT-domain-containing protein that retained two of the three tryptophan residues that constitute the tri-Trp cage was responsible for thalidomide binding to the domain, whereas the third tryptophan is replaced by another aromatic residue. Based on these findings, Danazumi et al. [10] have advocated for the exploration of IMid-based PROTACs as potential therapeutics against trypanosome infections. However, to date, no report has been made on an active molecule of this type.

A recent review byBurge et al. emphasizes that, although these enzymes may fulfill similar roles to those in model organisms, elucidating the specific ubiquitin transfer pathways—particularly the interactions among E1, E2, and E3 enzymes and their substrate proteins—remains a challenge [9]. The authors suggest that advances in structural biology, particularly through deep learning-based protein modeling, could be key to overcoming this barrier. In this report we combine experimental and state-of-the-art informatic structural biology methods to explore the real potential of using IMiD-based PROTACs on trypanosomatids. Our results warn of the real possibility that these compounds could successfully be developed.

2. Results

2.1. PROTAC dBET1 Exhibits the Same Trypanocide Activity as iBET JQ1 and Does Not Induce the Degradation of the T. cruzi Bromodomain Factor 3 (BDF3)

Trypanosoma cruzi, like the rest of the Trypanosomatids, possess genes encoding eight bromodomain proteins. We have previously described that two of these proteins, BDF1 and BDF3, are highly divergent members of the BET family [20]. Furthermore, we demonstrated the trypanocidal activity of two bromodomain inhibitors of this family (iBET151 and JQ1) and have associated this activity to at least one of these bromodomain proteins, TcBDF3 [21]. To evaluate the potential use of thalidomide-derived PROTAC compounds in trypanosomes, we compared the activity of the compound dBET1, a conjugate of JQ1 and TLD, with that of its separated components. dBET1 is a well-known PROTAC compound that targets BET family bromodomains and has shown activity in several experimental pathogenetic models such as glioblastoma, sepsis, and breast cancer, among others [22–24]. The same molar concentrations of TLD and JQ1+TLD in the same diluent were also used as controls. As shown in Figure 1A, dBET has a slightly higher activity than JQ1 against *T. cruzi* epimastigotes (a typical dose response curve is shown in Figure S1). Surprisingly, both TLD and the mixture of TLD and JQ1 showed higher trypanocidal activity than that of dBET1. When assayed in trypomastigotes, the trypanocide activities of JQ1 and dBET were also similar.

One of the problems observed in PROTAC compounds is that the chimeric molecules can decrease the affinity for their primary target. To explore this possibility, we measure the binding of dBET1 and JQ1 to recombinant BDF3 using a melting-point approach. As can be observed in Figure 1B, the affinities obtained for both compounds were similar. As a control, we used recombinant TcBDF2, which contains a bromodomain that does not belong to the BET family. As previously reported for JQ1 [25], neither this compound nor dBET1 showed affinity for TcBDF2 (Figures 1B and S2). This suggests that the slightly increased activity of dBET1 over JQ1 was due to TLD itself and not to a synergistic factor that could be due to the ubiquitination-mediated degradation of a bromodomain protein. To investigate this phenomenon in greater detail, we monitored by Western blot the presence of TcBDF3, a bromodomain protein that, as we know from previous studies, binds to JQ1 [21]. As can be

seen in Figure 1C, dBET1 did not induce the degradation of TcBDF3, even at concentrations well above the IC50.

A

compound	IC50 (Sy.x) µM	
	epimastigotes	trypomastigotes
JQ1	4.26 (0.07)	1.34 (0.03)
dBET1	2.11 (0.09)	5.55 (0.02)
JQ1+TLD	1.00 (0.19)	nd
TLD	0.17 (0.09)	nd

B

compound	Kd ± SD (µM)	
	TcBDF2	TcBDF3
JQ1	n.i.	45.7 ± 6.3
dBET1	n.i.	31.5 ± 4.9

C

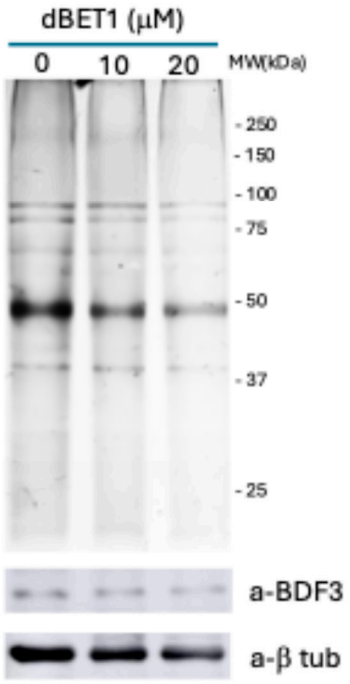

Figure 1. Activity of JQ1, dBET1, and TLD on *T. cruzi*. (**A**) IC50 of JQ1, dBET1, TLD, and JQ1+TLD on epimastigotes and trypomastigotes of *T. cruzi Dm*28c strain. nd: not detected. The table presents the IC_{50} values together with their corresponding Sy.x (standard deviation of the residuals), which is a statistical measure of the scatter of data points around a best-fit line or curve in a regression analysis. Data correspond to one representative experiment from three independent experimental replicates, n.i.: no inhibition. A typical dose response curve is shown in Figure S1. (**B**) Dissociation constant (K_d) of JQ1 and dBET1 on TcBDF2 and TcBDF3. A typical melting curve at different concentrations of each compound is shown in Figure S2. (**C**) Total proteins were evaluated via Coomasie staining and Western blot detection of TcBDF3 and a-tubulin from parasites incubated with different concentrations of dBET1. The figure represents one of two assays performed independently with similar results.

These results clearly indicate that dBET1 is not active as a PROTAC compound, but they do not completely rule out the possibility that this type of compound may fail to function in *T. cruzi*. The lack of activity observed could be due to the small size of the linker between JQ1 and TLD or to the parasite's low permeability for the compound. Furthermore, the slightly higher trypanocidal activity of TLD compared to dBET1, in addition to being a reflection of the lack of functional PROTAC activity in *T. cruzi*, could be due to a combination of better physicochemical properties and possible off-target effects of TLD in parasite-specific pathways.

There are a variety of PROTAC inhibitors derived from JQ1 and TLD that could be tested in the future, but the question arises as to how many negative results would be necessary (and sufficient) to confirm that TLD-derived PROTAC compounds are not functional in trypanosomatids. As an alternative to this experimental "tour de force" approach, we decided to critically evaluate the assumption that trypanosomatids possess a functional $CRL4^{CRBN}$ that makes the use of TLD-derived PROTAC compounds possible by using in silico structural tools.

2.2. The E3 Ubiquitin Ligase CRL4^{CRBN} Is Not Completely Conserved in T. cruzi

Considering the results obtained with the dBET1 compound, we conducted a detailed search for potential components of the CRL4^{CRBN} complex in *T. cruzi* using both sequence (BLAST, 2.17.0+, TritrypDB, https://academic.oup.com/nar/article/52/D1/D808/7416377, accessed on 28 April 2025) and structural (FoldSeek, https://www.nature.com/articles/s41587-023-01773-0, accessed on 28 April 2025) alignment methods. For this, we used as query the human components of CRL4^{CRBN}, hereafter named *Hs*RBX1, *Hs*Cul4B, *Hs*DDB1, and *Hs*CRBN. Results are summarized as follows:

CRBN: Sequence and structural similarity analyses identified the previously described *T. cruzi* protein containing a CULT domain. This protein, TcCLB.508777.70, hereafter referred to as *Tc*CRBN-like, comprises 209 amino acids and is less than half the size of human CRBN (442 amino acids). Structural similarity is confined to the CULT domain (residues V39 to D190), which corresponds to the C-terminal half of metazoan CRBNs. At the putative IMiD-binding site, *Tc*CRBN-like has one of the three highly conserved tryptophanes replaced by phenylalanine. *Tc*CRBN-like lacks the N-terminal LON domains present in *Hs*CRBN, which are essential for binding to DDB1. No *T. cruzi* protein was found with LON domains or with sequence or structural similarity to the first 350 amino acids of human CRBN.

Trypanosomatids' CRBN homologs share around 35% sequence identity among them, primarily within the CULT domain. *T. brucei* and *L. major* CRBN-like proteins (Tb927.11.12580 and LmjF.09.0570) are longer than TcCRBN-like toward the C-terminus (393 and 492 AA, respectively) and they all lack LON domains.

Two *T. cruzi* sequences with similarity to metazoan DDB1 were identified. The one identified by BLAST, TcCLB.510643.130 (774 AA), is shorter than human DDB1 (1140 AA) and shares 25% of its global sequence similarity. Compared with DDB1, it lacks the first beta-propeller RSE1 domain at its N-terminus. It was annotated as a putative damage-specific DNA-binding (DDB) protein. The one identified by FoldSeek, TcCLB.506871.140 (1436 AA), shows a 32% global sequence identity and greater structural similarity to *Hs*DDB1. This protein has the same domain architecture as DDB1 and was annotated as Cleavage and Polyadenylation Specificity Factor subunit 1 (CPSF1). Both sequences have homologs in *T. brucei* and *Leishmania* spp.

Two *T. cruzi* sequences were identified as top candidates in sequence and structural comparisons with human CUL4A (913 AA) using BLAST, TcCLB.503813.20 (909 AA), and FoldSeek, TcCLB.511075.40 (741 AA). Both proteins are clearly members of the cullin family. The shorter protein lacks an ortholog in *T. brucei*, while the larger protein has orthologs in both *T. brucei* and *Leishmania* spp. and has been annotated as a putative CUL4B. Among the several previously identified members of the cullin family, these are the trypanosomatid proteins most similar to vertebrate CUL4B.

The top hit in both sequence similarity and structural similarity searches for human RBX1 was TcCLB.506495.9, annotated as a putative RING-H2 zinc finger protein, sharing 63.21% of its identity with human RBX1. Clear orthologs were identified in other trypanosomatids, exhibiting over 70% sequence similarity among then. The *T. brucei* homolog RBX1 was previously characterized [16]. These sequences clearly correspond to the member of the RING family proteins most similar to RBX1. Notably, the *T. cruzi* TcCLB.506495.9 sequence (from the CL Brener non-Esmeraldo reference strain) is 152 amino acids long, whereas orthologs in *T. brucei*, *Leishmania* spp., and other *T. cruzi* strains are 106 amino acids in length, closely matching the size of human RBX1 (108 AA). Detailed inspection of the N-terminal region suggests that the extended length of the CL Brener sequence likely results from a misassignment of the start methionine during genome annotation. The domain architectures of *Hs*RBX1, *Hs*Cul4B, *Hs*DDB1, and *Hs*CRBN and their homolog

candidates from *T. cruzi* are shown in Figure 2A and a summary of information about all the sequences used in this study can be found in Table S1.

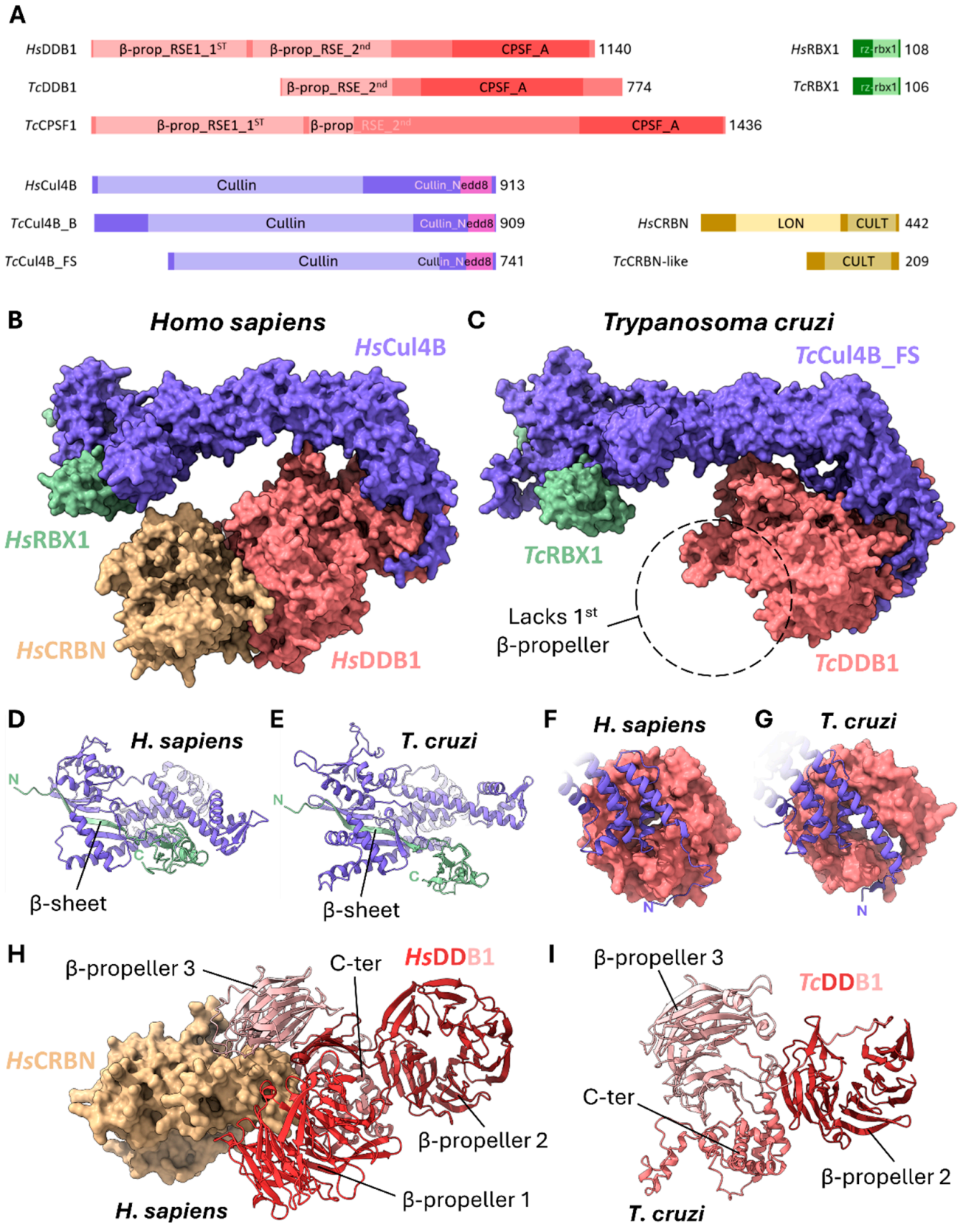

Figure 2. Structural comparison between *Homo sapiens* and *Trypanosoma cruzi* E3L complexes. (**A**) Detected InterPro domains of *Homo sapiens* (*Hs*) E3L components and their potential homologs

from *T. cruzi* (*Tc*). (**B**) Solvent exposed surface of the convergent complex structure of *H. sapiens* E3L predicted using MultimerMapper. Protein names and color hues match those in panel A. (**C**) Solvent exposed surface of the convergent complex structure of *T. cruzi* E3L predicted using MultimerMapper and aligned to the structure from panel B. The lack of the first β-propeller of *Tc*DDB1 compared to *Hs*DDB1 is highlighted. (**D**) Predicted interaction between *Hs*RBX1 and *Hs*Cul4B from the *H. sapiens* complex compared with the predicted interaction between *Tc*RBX1 and *Tc*Cul4B_B (**E**). Both *Hs*RBX1 and *Tc*RBX1 introduce their N-terminal segments into the head of their corresponding Cul4B to form a β-sheet. (**F**) Predicted interaction between *Hs*Cul4B and *Hs*DDB1 compared with the predicted interaction between *Tc*Cul4B_B and *Tc*DDB1 (**G**). Both Cul4B proteins interact through a non-structured N-terminal segment and their globular domains over the second β-propeller of their corresponding DDB1. (**H**) Predicted interaction between *Hs*DDB1 and *Hs*CRBN. Different structural features are highlighted. The β-propellers 1 and 3 hold on to *Hs*CRBN from two sides. The C-terminal segment of *Hs*DDB1 is partially visible behind β-propeller 1. (**I**) Predicted structure of *Tc*DDB1. Notice the lack of the first β-propeller compared to *Hs*DDB1.

Sequence analyses thus identify clear candidates from the RING and cullin protein families that could participate in a CRL4-like complex in trypanosomatids. However, the incomplete conservation of CRBN orthologs raises questions about the existence of a fully functional ortholog of the $CRL4^{CRBN}$ complex in these organisms. To further explore the potential formation of a CRBN–DDB1–RBX1–CUL4B tetramer in *T. cruzi*, we modeled the structures of the identified candidate proteins using AlphaFold3 [26] modeling combined with statistical analysis using MultimerMapper [27]. Briefly, MultimerMapper analyzes protein structure prediction ensembles modeled using different combinations of input protein entities to predict interactions and the formation of stable complexes within an input system. It analyzes increasingly larger combinations of subunits by exploring the stoichiometric space to find the most likely combinations of proteins and the stoichiometric coefficients that form stable complexes inside the system under analysis. MultimerMapper was trained on a curated dataset of experimentally validated trypanosomatid protein–protein interactions collected from the literature. The whole output files and structure explored files are available at the CONICET Data Repository (http://hdl.handle.net/11336/273301).

When MultimerMapper is applied to the system that contains the protein entities *Hs*RBX1, *Hs*Cul4B, *Hs*DDB1, and *Hs*CRBN, it converges in the complex from Figure 2B, which has the expected stoichiometry 1:1:1:1 [28]. The results of the stoichiometric space exploration algorithm can be found in Figure S1A. The convergent structure displays all the features of an E3L complex when compared to the closest available E3L complex RBX1-Cul4A-DDB1-SV5V deposited in the Protein Data Bank (Figure S3). On the other hand, the same pipeline was applied for the system consisting of *Tc*RBX1, *Tc*Cul4B_B, *Tc*Cul4B_FS, *Tc*DDB1, *Tc*CPSF1, and *Tc*CRBN-like. In contrast, the execution converges in a 1:1:1 complex consisting of just *Tc*RBX1, *Tc*Cul4B_FS, and *Tc*DDB1 (Figures 2A and S4A). It is worth noticing that *Tc*CPSF1 does not interact with any protein from the input system and another 1:1 subcomplex consisting of *Tc*Cul4B_B and *Tc*RBX1 is also formed. However, only *Tc*CUL4B_FS is included in the complex together with *Tc*DDB1, suggesting that *Tc*CUL4B_B could be part of another ligase together with *Tc*RBX1. It is also plausible to think that *Tc*CUL4B_FS is the homolog of human *Hs*CUL4A. Also, in addition to interacting with itself, *Tc*CRBN-like is predicted to exist outside of the protein–protein interaction (PPI) network that contains *Tc*RBX1, *Tc*Cul4B_FS, and *Tc*DDB1 (Figure S4B).

The structure of the convergent 1:1:1 complex is shown in Figure 2C and is highly similar to the human complex (Figure 2B), but with key differences. The interaction between RBX1 and Cul4B is conserved in both complexes (Figure 2D,E), consisting of RBX1 extending its N-terminal segment over the head of Cul4B to form a β-sheet, a characteristic feature of many E3L complexes [28,29]. Another conserved feature is the interaction mode

between Cul4B and DDB1, where both Cul4B proteins interact through an unstructured segment and part of their globular segment with the second β-propellers of DDB1 [1]. However, the interaction between CRBN and DDB1 is absent in *T. cruzi*. In humans, the interaction between *Hs*CRBN and *Hs*DDB1 is mediated mainly through the first β-propeller of *Hs*DDB1, complemented by interactions through its third β-propeller, which holds the LON domain of *Hs*CRBN from two sides (Figure 2H). Meanwhile, *Tc*DDB1 conserves many features of *Hs*DDB1, like the C-terminal domain (Figure S5), but importantly, it lacks the first β-propeller (Figure 2I), an essential element to interact with CRBN. As mentioned, the only potential homolog of *Hs*CRBN, *Tc*CRBN-like, lacks the LON domain (Figure 2A).

These results raise serious doubts about the presence of a structurally and functionally orthologous $CRL4^{CRBN}$ complex in trypanosomatids. While there are orthologs of DDB1, CUL4B, and RBX1 that are likely components of E3 ubiquitin ligase complexes, the absence of a detectable interaction between CRBN-like and DDB1, which is critical for canonical $CRL4^{CRBN}$ assembly, suggests this complex is not fully conserved. Similar observations were seen when the same pipeline was applied using *T. brucei* and *L. major* sequences (Table S1), where *Tb*CRBN-like and *Lm*CRBN-like were detected outside their respective PPI networks in all the tested modeling conditions (Figure S6). It is worth noting that no interaction was observed between CRBN-like and any of the DDB1 homologues of these organisms, even though all of them possess the first β-propeller domain.

2.3. The CRBN Homologous Protein in T. cruzi Has a Small Pocket That Cannot Contain IMids

It has been suggested that CRBN can participate as a chaperone, in a TLD-interfered ubiquitination-independent process. In this context, it is conceivable that a *Tc*CRBN-like protein might mediate the parasite IMiD-sensitive process in the context of a widely divergent E3 ligase or even without the participation of any E3 ligase. If such a scenario exists, the interaction between *Tc*CRBN-like and IMiDs via the CULT domain pocket would be essential for the functional activity of a PROTAC compound. As previously noted, this interaction has generally been inferred in the literature for all proteins containing a CULT domain, primarily based on sequence similarity and homology modeling. Since recombinant TcCRBN-like protein is not available for TLD interaction assays, we analyzed the binding cavity of both human and *T. cruzi* CULT domains using the same molecular dynamics (MD) protocol. We performed 1000 ns MD simulations and clustered the conformations based on the position of three key aromatic residues within the binding pocket.

For the human CRBN CULT domain, during MD simulations, two distinct conformations emerged: one with a closed pocket (74% frequency) and one with an open pocket (26% frequency). The pocket was closed by a W386 adjustment that rotated at an angle of ~50° to seal the cavity (Figures 3A,B and S7). In docking simulations, the open pocket's size was able to accommodate thalidomide, lenalidomide, and pomalidomide in a similar position to that observed in analogous CRBN crystallographic structures (Figures 3E,F and S8) [30,31]. Similarly, the TcCRBN-like CULT domain also exhibited closed and open pocket conformations, with frequencies of 91% and 10%, respectively (Figure 3C,D). In this case, it was the W93 that clogged the pocket. However, its pocket was shallower and docking studies confirmed that it could not accommodate thalidomide, lenalidomide, or pomalidomide (Figures 3G,H and S5). During MD simulations, no significant mobility of the CULT domain relative to the first LON subdomain was observed, as has been reported in other experimental models. This talidomide-dependent folding was well characterized in the CRBN-like MsCI4 from *Magnetospirillum gryphiswaldense* [32], but the allostery of drug-induced neosubstrate on human CRBN binding remains as of yet

unclear. It is worth noting that other previous MD simulation studies on human CRBN have also been unable to capture this mobility [33–35]. In sum, our results suggest that TcCRBN-like cannot bind TLD, indicating that the trypanocide activity of this compound is not due to the interaction with its CULT domain, raising an intriguing question about this activity.

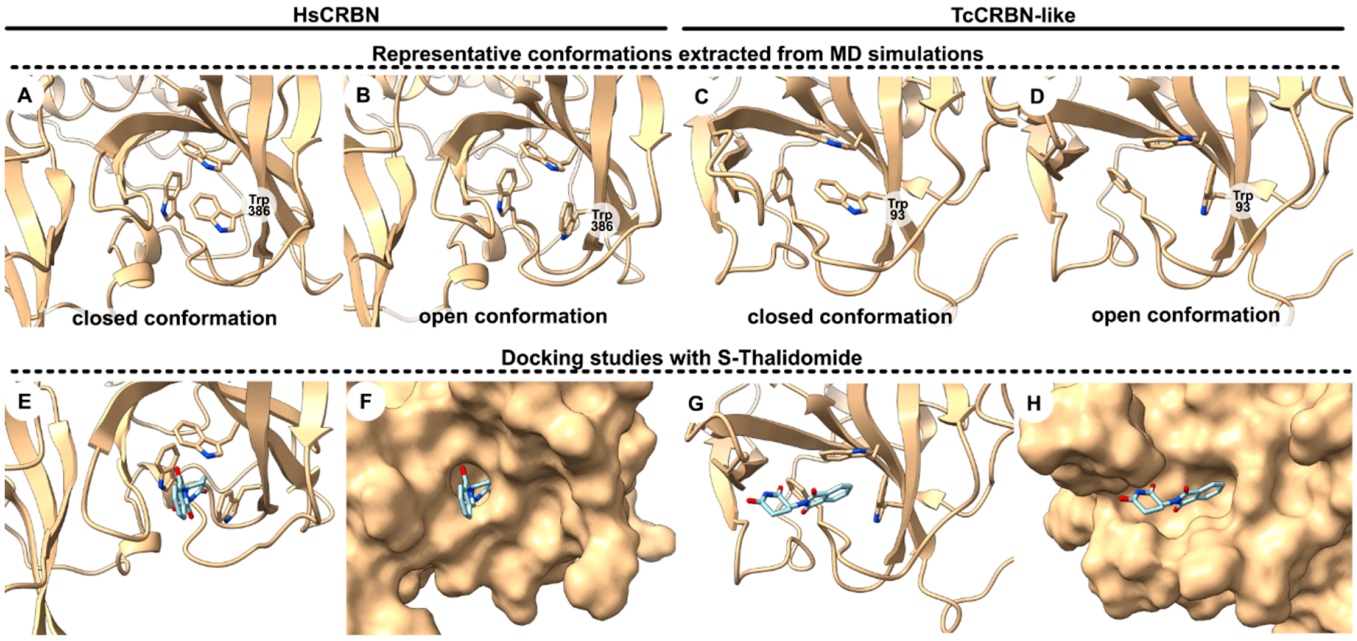

Figure 3. Representative structures obtained from MD simulations of (**A**) closed conformation of HsCRBN, (**B**) open conformation of HsCRBN, (**C**) closed conformation of TcCRBN-like, (**D**) open conformation of TcCRBN-like. Docking poses of S-Thalidomide in (**E**) HsCRBN (in cartoon representation), (**F**) HsCRBN (in surface representation), (**G**) TcCRBN-like (in cartoon representation), (**H**) TcCRBN-like (in surface representation). S-Thalidomide and key residues of the active site are represented in licorice (C atoms of S-Thalidomide are depicted in ligh blue and C atoms of the protein are depicted in ochre).

3. Discussion

The results presented here, although not definitive, clearly suggest that trypanosomatids do not possess a $CRL4^{CRBN}$-type E3 ligase that could be targeted by PROTAC-type compounds designed with IMiDs. Looking at the mechanisms in which $CRL4^{CRBN}$ is involved in other organisms, which potentially exist in Trypanosomatids, could help us to better understand the situation..

Several proteins physiologically capable of interacting with CRBN and subsequently being targeted to the proteasome via $CRL4^{CRBN}$ have been described so far. Among them, the best characterized are BKCa channel α subunit, chloride channel protein CLC-1 and the transcription factors c-Jun, Ikaros (IKZF1), Aiolos (IKZF3), embryonic transcription factor SALL4, and homeodomain-containing factor MEIS2 [36,37]. Of these, only MEIS2 shares a binding site with IMiDs and its degradation in the proteasome is inhibited by these compounds [38]. In the other cases, the presence of IMiDs does not modify or even increase degradation by the proteasome. CRBN also interacts with the zinc finger domain of TNF receptor-associated factor 6 (TRAF6) and prevents the formation of polyubiquitin chains on TRAF6 and TAK1-binding protein 2 (TAB2), leading to the suppression of inflammation [39]. It was also discovered that CRBN interacts with p62 and prevents its association with polyubiquitinated proteins, thus reducing protein aggregates formed under proteasomal stress and protecting neuronal cells from pathological mutation-induced cell

death [40]. Finally, CRBN has also been associated with the ubiquitination and proteolysis of amyloid precursor protein (APP) by a binding mode completely independent of the CULT domain [41]. So far, beyond those related to the autophagocytic system, none of these proteins have identifiable orthologs in trypanosomatids. Moreover, since trypanosomatids lack these regulatory pathways and do not possess conventional transcription factors, it is reasonable to assume that the function of TcCRBN-like is not associated with the aforementioned proteins.

It has also been established that the binding patterns of CRBN to thalidomide and uridine are similar, and it has recently been proposed that C-terminal aspartimide and aminoglutarimide residues resulting from protein damage and chain breaks are the native degrons of CRBN [42–44]. Although this hypothesis about the physiological function of the CULT domain of CRBN as a receptor for the degradation of damaged proteins is far from being conclusively proven, to date it is the only one that can be extrapolated beyond the metazoans that possess a canonical CRBN.

Ubiquitin E3 ligases constitute a highly diverse class of multiprotein complexes, typically assembled from three to five components drawn from a broad repertoire of proteins grouped into five major families. In trypanosomes, Gupta et al. identified a substantial number of putative E3 ligase components (109 in *T. cruzi*), although this number remains markedly lower than in humans, where more than 800 E3 ligases have been described [17]. Among the trypanosome repertoire, at least 13 members belong to the cullin family. CUL4, together with CUL1 and CUL3, are considered the phylogenetically oldest and most deeply rooted proteins [45]. In our work, we identified proteins with similarity to DDB1, CRX1, and CUL4, which are likely constituents of at least one CRL4-type E3 ligase complex. In mammalian systems, CRBN functions as one of over 100 potential substrate receptors for these complexes, collectively termed DCAFs (DDB1- and CUL4-associated factors) [6]. DCAFs are known to regulate, via ubiquitination and further degradation of specific target proteins, a broad range of cellular processes, including transcription, cell cycle progression, DNA repair, and the maintenance of genomic stability [3,6,45]. The primary objective of our study was not to characterize the DCAF repertoire of this complex, but rather to assess the potential activity of CRBN-like receptors. Nonetheless, it is important to note that trypanosomatids harbor a considerable number of putative DCAF orthologs that could serve as substrate receptors in these complexes. The DDB1–CUL4A ubiquitin ligases are essential for maintaining genomic integrity in organisms from yeast to mammals, using WD40-repeat domain-containing proteins as receptors bound to DDB1 [46,47]. However, even though there exist more than 100 proteins sharing WD40 repeats coded in Trypanosomes' genomes, experimental characterization of cullin complexes in *T. brucei* did not reveal receptor proteins with these domains [19]. Computational approaches such as those employed in this study provide a powerful means to predict and analyze the composition and potential activities of such complexes in the future.

4. Materials and Methods

4.1. Chemical Compounds

(+)-JQ1 (CAT No.: B0084-453787) and dBET1 (CAT No.: BP-400006) were provided by BOC Sciences®, New York, NY, USA. Thalidomide comes from Laboratorio Lazar, Buenos Aires, Argentina.

4.2. Trypanocide Assay

T. cruzi Dm28c that expresses the *Escherichia coli* LacZ gene epimastigotes were cultured and obtained as previously described [48,49]. The compounds were dissolved in dimethyl sulfoxide (DMSO) with a final concentration of the solvent < 1%. DMSO 1% was used as

a control to evaluate solvent toxicity and Benznidazol in the same solvent as a positive control. Quadruplicates were run in the same microplate and repeated in three experiments. The half-maximal inhibitory concentration (IC_{50}) values were calculated using non-linear regression on GraphPad prism 9.0 as previously described [49]. In the fitted curves used to calculate IC50 values, we report standard deviations of the residuals (Sy.x) as the standard error of the estimation of one representative experiment. The assays were repeated at least three times with no significant variation in IC50 values for each life cycle stage.

4.3. Recombinant Protein Purification

As previously reported, TcBDF3 were purified from inclusion bodies [21]. Briefly, pDEST17-TcBDF3 and TcBD3 were transformed into *E. coli* BL21, and recombinant proteins (fused to a His tag) were obtained by induction with 0.1 mM isopropyl-β-D-thiogalacto-pyranoside (IPTG) overnight at 22 °C. The protein was purified from the inclusion bodies, and the solubilized proteins were dialyzed against 0.1 mM phosphate buffer pH 8. TcBD2 was purified under soluble conditions as reported previously from *E. coli* BL21 transformed with pDEST17-TcBD2. The recombinant protein was obtained by induction with 0.5 mM IPTG for 3 h at 37 °C [50]. The recombinant protein was purified using a nickel-charged resin (Ni-NTA Agarose, Qiagen, Germantown, MD, USA) following the manufacturer's instructions. Correct folding was verified by Circular Dichroism spectroscopy using a spectropolarimeter (Jasco J-810, JASCO Corporation, Easton, MD, USA).

4.4. Thermal Shift Assay

Recombinant TcBDF3 and TcBDF2 were buffered in 10 mM HEPES, pH 7.5, and 500 mM NaCl and assayed in a 48-well plate at a final concentration of 2 μM in 20 μL volume. Compounds (JQ1 and dBET1) were added at a final concentration between 1 and 200 μM to calculate dissociation constants. SYPRO Orange (Invitrogen, Waltham, MA, USA) was added as a fluorescence probe at a dilution of 1:1000. Excitation and emission filters for SYPRO Orange dye were set to 465 and 590 nm, respectively. The temperature was raised with steps of 2 °C per minute from 25 °C to 96 °C, and fluorescence readings were taken at each interval in a CFX Opus 96 Real-Time System and analyzed using the Maestro Software 2.3 (Biorad, Hecules, CA, USA). The melting curves and average melting temperature for each condition were obtained and plotted in temperature vs. concentration graphs in GraphPad Prism 9.0. Plots were fitted using the DSF single binding site equation to obtain the dissociation constants (*Kd*).

4.5. Western Blot

Protein extracts (~30 μg) were separated by SDS-PAGE and transferred to nitrocellulose membranes. The transferred proteins were visualized with Ponceau S. The membranes were treated with 10% non-fat milk in PBS for 2 h and then incubated with specific antibodies diluted in PBS for 3 h. The antibody used were polyclonal rabbit anti-TcBDF3 [21] and monoclonal antibody against a-tubulin (ThermoFisher, Waltham, MA, USA # 32-2500). Bound antibodies were detected using peroxidase-labeled anti-mouse (GE Healthcare, Chicago, IL, USA) or anti-rabbit (Pierce, Rockford, IL, USA) goat IgGs and ECL Prime (GE Healthcare) according to the manufacturer's protocol.

4.6. Structural Modeling

Potential orthologous sequences for each component of the $CRL4B^{CRBN}$ complex from *Trypanosoma cruzi*, *Trypanosoma brucei*, and *Leishmania major* were identified using BLAST searches in TriTrypDB [51] and FoldSeek webtool [52], with the human components sequences of the complex (Q96SW2, Q16531, P62877, Q13620) serving as queries. Protein domains were identified using MOTIF Search (https://www.genome.jp/tools/motif/,

accessed on 28 April 2025). Global protein pair alignments were performed using the Needleman–Wunsch algorithms implemented into BLAST suite [53].

Each protein system was analyzed using AlphaFold3, aided with the suggestion of protein combinations for structural modeling generated by MultimerMapper (https://github.com/elviorodriguez/MultimerMapper). The structures of the combination suggestions between the sequences were predicted using AlphaFold3 server [25] and transformed to a MultimerMapper compatible format with the af3_compatibility.py utility from MultimerMapper. Initially, all possible 2-mer combinations (including homodimers) were predicted and provided to MultimerMapper to detect stable pairs. For every stable pair (parent), 3-mer combination suggestions were generated by adding one subunit of each possible protein entity of the system (children). These 3-mer suggestions were then predicted and provided to MultimerMapper to detect stable stoichiometries and suggest new sets of protein combinations (4-mers). The process was repeated iteratively until the N-mer iteration at which no more stable combinations were detected. Executions were performed at a false positive rate of 0.01 (minimum interaction PAE of 10 Å and 5 models as cutoffs). For each branch of the parent–child hierarchy (stoichiometric space), the highest combination of proteins that gave rise to a stable complex was considered as a convergent stoichiometry.

For the modeling of the human CRL4B^{CRBN} complex, the aforementioned human sequences were used. To explore the hypothetical structure of TcCRL4B, the top candidate sequences identified by BLAST and FoldSeek were employed: TcCLB.508777.70, TcCLB.510643.130, TcCLB.506871.140, TcCLB.506495.9, TcCLB.511075.40, and TcCLB.503813.20. The same process was performed with *Trypanosoma brucei* and *Leishmania major* orthologs, as indicated in the Supplementary Materials (Figure S6).

4.7. Molecular Dynamics Simulations and Docking

Molecular dynamics (MD) simulations were performed using Amber24 software [54]. The starting structure of HsCRBN and TcCRBN-like were obtained using AlphaFold3 (see above). The proteins were first immersed in a periodical octahedral box of TIP3P water molecules [55]. The ff14sb force field was employed for proteins. The structures were then optimized, taken from 0 to 300 K at constant volume for 25 ps, equilibrated at a constant pressure of 1 bar for 25 ps, and finally subjected to 1000 ns of production simulation using PMEMD CUDA software 24.0 implemented in Amber24 with the FF14SB forcefield [56]. Temperature control was performed using the Langevin thermostat, and pressure control using the Monte Carlo barostat. Clustering analyses were performed with cpptraj, applying hierarchical agglomerative clustering to 1000 frames sampled from the MD trajectories. Mass-weighted RMSD values were computed over residues 380, 386, and 400 in HsCRBN, and residues 87, 93, and 107 in TcCRBN-like, with the number of clusters fixed to two [57].

Docking studies were carried out using the OpenEye OEDocking suite with FRED 4.3.1.0 performing rigid-body docking of ligand libraries into the prepared receptor structures. Top-ranked poses were selected according to the Chemgauss4 scoring function [58].

5. Conclusions

Our results raise significant doubts on the functionality of thalidomide-based PROTACs in trypanosomatids. Moreover, they also challenge the widely accepted notion that the CULT domain inherently serves as an interaction site for IMiDs. In fact, there is no experimental evidence to justify the presumption that proteins with the CULT domain are part of some type of E3 ubiquitin ligase outside of metazoans that possess a canonical

CRBN. Furthermore, since the physiological ligands of the CULT domain remain partially unknown, it is worth questioning whether the pocket through which some CULT domains bind IMiDs is truly essential for the function of all CULT domain-containing proteins. Unfortunately, a thorough reading of the literature shows that the idea that the presence of a CULT domain implies binding to IMiDs is so deeply rooted that any protein with a CULT domain is often referred to as a cereblon isoform. This overgeneralization and simplification of the function of the CULT domain have led to claims that PROTAC compounds derived from IMiDs can be functional in any organism that has a protein with this domain. In this sense, it may be speculated that the evolutionary conservation of certain amino acids involved in IMiDs binding could reflect a structural role necessary for maintaining the proper folding of the domain, rather than the formation of a functional binding pocket directly related to the domain's biological activity.

The results presented herein emphasize the necessity of integrating functional and structural validation in drug discovery and show that current available in silico tools like those derived from the development of AlphaFold can be helpful for exploring structural/functional conservation among distant species.

Finally, despite the questions we raised regarding the existence of a functional homolog of $CRL4^{CRBN}$ in trypanosomatids, it is necessary to highlight that the development of PROTAC compounds against these organisms still holds great potential. Recently, a comprehensive review on this topic was published [13]. In that publication, the authors propose a pipeline for the development of TrypPROTAC compounds with a novel rationale. This pipeline does not focus on designing compounds based on an established binder (such as IMiDs) but rather proposes a comprehensive exploration of known target inhibitors, a broad group of E3 ligases, and chemical characteristics of the compounds (such as the type of linker that joins the two functional molecules). Furthermore, beyond classical PROTACs, other alternative degradation strategies, such as molecular adhesives, homoPROTACs, and Lysosome-Targeting Chimera (LYTAC) compounds, could also be novel approaches for the development of new trypanocide compounds.

Supplementary Materials: The following supporting information can be downloaded at: https://www.mdpi.com/article/10.3390/ddc4040055/s1. Table S1. Summary of sequences used in the study. Figure S1. Dose-dependent viability curve for the different compounds tested. Figure S2. Differential scanning fluorimetry of TcBDF2 and TcBDF3 with JQ1(+) and dBET1. Figure S3. Predicted stoichiometry for the human E3L complex. Figure S4. MultimerMapper results for the system containing the *T. cruzi* proteins. Figure S5. Structural alignment of the C-terminal domains of HsDDB1 and TcDDB1. Figure S6. Predicted PPI networks for E3L from other Trypanosomatids. Figure S7. Analysis of Trp385 (HsCRBN) and Trp93 (TcCRBN-like) position during molecular dynamics. Figure S8. Docking of lenalidomide and pomalidomide on HsCRBN and TcCRBN-like.

Author Contributions: Conceptualization, E.S., V.L.A. and D.M.M.; software, E.R.A.; validation, E.S. and D.M.M.; formal analysis, E.S., E.R.A., G.F., R.M. and V.L.A.; investigation, R.M., V.L.A., V.B., G.F., G.R.B. and E.S.; resources, G.R.B.; writing—original draft preparation, E.S.; writing—review and editing, E.S., V.L.A., E.R.A. and D.M.M.; visualization, E.R.A. and G.F.; supervision, E.S. and D.M.M.; funding acquisition, E.S. All authors have read and agreed to the published version of the manuscript.

Funding: E.S. and V.A.L. are researchers, and V.B., G.F., and G.R.B. are fellows at the National Research Council (CONICET). This work was funded by Agencia Santafesina de Ciencia Tecnología e innovación, Santa Fe, Argentina (ASACTEI) (PEICID-2022-136).

Data Availability Statement: The data corresponding to the structural analysis of the CRL4 complexes are available in the CONICET Data Repository http://hdl.handle.net/11336/273301, accessed on 28

April 2025. MultimerMapper is available at https://github.com/elviorodriguez/MultimerMapper, accessed on 28 April 2025.

Acknowledgments: We are grateful to Javier Jalife for their excellent technical assistance.

Conflicts of Interest: The authors declare no conflict of interest.

Abbreviations

APP	Amyloid Precursor Protein
BET	Bromodomain and Extra-Terminal domain
BKCa	BK Channel alpha Subunit (Calcium-activated Potassium Channel Subunit alpha-1)
cIAP1	Inhibidor de Apoptosis Celular 1
CLC-1	Chloride Channel Protein 1
CRBN	Cereblon Protein
CRL4-E3L	Cullin-RING type E3 Ligase
CRL4	Cullin-4-based RING Ubiquitin Ligase
$CRL4^{CRBN}$	Cereblon-containing Cullin-RING Ubiquitin Ligase
CUL4A/4B	Cullin-4A/B
CULT	Cereblon Domain of Unknown Activity
DCAFs	DDB1- and CUL4-associated Factors
DDB1	Damaged DNA Binding Protein 1
E1	Ubiquitin-activating Enzyme
E2	Ubiquitin-conjugating Enzyme
E3	Ubiquitin Ligase Enzyme
IKZF1	Ikaros Zinc Finger Transcription Factor
IKZF3	Aiolos Zinc Finger Transcription Factor
IMiDs	Immunomodulatory Imides
LON domain	ATP-dependent Protease La Domain
LYTAC	Lysosome-Targeting Chimera
MD	Molecular Dynamics
MDM2	Murine Doble Minute 2
MEIS2	Meis (Myeloid Ecotropic Viral Integration Site) Homeobox 2
p62	protein adaptor connecting ubiquitinated proteins for degradation through autophagy or the ubiquitin-proteasome system
PROTAC	Proteolysis Targeted Chimeras
RBX1	RING Box 1 protein
ROC1	Regulator of Cullins 1
SALL4	Sal-Like Protein 4 (embryonic transcription factor)
TAB2	TAK1(Transforming Growth Factor beta-Activated Kinase 1)-Binding Protein 2
TcBDF2	*T. cruzi* Bromodomain Factor 2
TcBDF3	*T. cruzi* Bromodomain Factor 3
TLD	Thalidomide
TRAF6	TNF Receptor-Associated Factor 6
VHL	von Hippel-Lindau protein
WD40-repeats	short structural motif of approximately 40 amino acids, often terminating in a tryptophan-aspartic acid (WD) dipeptide

References

1. Sakamoto, K.M.; Kim, K.B.; Kumagai, A.; Mercurio, F.; Crews, C.M.; Deshaies, R.J. Protacs: Chimeric Molecules That Target Proteins to the Skp1-Cullin-F Box Complex for Ubiquitination and Degradation. *Proc. Natl. Acad. Sci. USA* **2001**, *98*, 8554–8559. [CrossRef]
2. Békés, M.; Langley, D.R.; Crews, C.M. PROTAC Targeted Protein Degraders: The Past Is Prologue. *Nat. Rev. Drug Discov.* **2022**, *21*, 181–200. [CrossRef]

3. Tanaka, K.; Suzuki, T.; Chiba, T. The Ligation Systems for Ubiquitin and Ubiquitin-like Proteins. *Mol. Cells* **1998**, *8*, 503–512. [CrossRef] [PubMed]
4. Gu, S.; Cui, D.; Chen, X.; Xiong, X.; Zhao, Y. PROTACs: An Emerging Targeting Technique for Protein Degradation in Drug Discovery. *BioEssays News Rev. Mol. Cell. Dev. Biol.* **2018**, *40*, e1700247. [CrossRef] [PubMed]
5. Jackson, S.; Xiong, Y. CRL4s: The CUL4-RING E3 Ubiquitin Ligases. *Trends Biochem. Sci.* **2009**, *34*, 562–570. [CrossRef]
6. Jang, S.-M.; Redon, C.E.; Aladjem, M.I. Switching DCAFs: Beyond Substrate Receptors. *BioEssays News Rev. Mol. Cell. Dev. Biol.* **2021**, *43*, e2100057. [CrossRef]
7. Miyauchi-Nanri, Y.; Mukai, S.; Kuroda, K.; Fujiki, Y. CUL4A-DDB1-Rbx1 E3 Ligase Controls the Quality of the PTS2 Receptor Pex7p. *Biochem. J.* **2014**, *463*, 65–74. [CrossRef]
8. Lupas, A.N.; Zhu, H.; Korycinski, M. The Thalidomide-Binding Domain of Cereblon Defines the CULT Domain Family and Is a New Member of the β-Tent Fold. *PLoS Comput. Biol.* **2015**, *11*, e1004023. [CrossRef]
9. Burge, R.J.; Mottram, J.C.; Wilkinson, A.J. Ubiquitin and Ubiquitin-like Conjugation Systems in Trypanosomatids. *Curr. Opin. Microbiol.* **2022**, *70*, 102202. [CrossRef] [PubMed]
10. Danazumi, A.U.; Ishmam, I.T.; Idris, S.; Izert, M.A.; Balogun, E.O.; Górna, M.W. Targeted Protein Degradation Might Present a Novel Therapeutic Approach in the Fight against African Trypanosomiasis. *Eur. J. Pharm. Sci. Off. J. Eur. Fed. Pharm. Sci.* **2023**, *186*, 106451. [CrossRef]
11. Espinoza-Chávez, R.M.; Salerno, A.; Liuzzi, A.; Ilari, A.; Milelli, A.; Uliassi, E.; Bolognesi, M.L. Targeted Protein Degradation for Infectious Diseases: From Basic Biology to Drug Discovery. *ACS Bio Med Chem Au* **2023**, *3*, 32–45. [CrossRef]
12. Hasslocher-Moreno, A.M. Trypanocidal Treatment for Chronic Chagas Disease: Past, Present, and Future. *Rev. Soc. Bras. Med. Trop.* **2025**, *58*, e02422025. [CrossRef]
13. Rodriguez Gini, A.L.; Souza Tada da Cunha, P.; João, E.E.; Man Chin, C.; dos Santos, J.L.; Serra, E.C.; Benito Scarim, C. TrypPROTACs Unlocking New Therapeutic Strategies for Chagas Disease. *Pharmaceuticals* **2025**, *18*, 919. [CrossRef] [PubMed]
14. Hashimoto, M.; Murata, E.; Aoki, T. Secretory Protein with RING Finger Domain (SPRING) Specific to Trypanosoma Cruzi Is Directed, as a Ubiquitin Ligase Related Protein, to the Nucleus of Host Cells. *Cell. Microbiol.* **2009**, *3*, 32–45.
15. Muñoz, C.; San Francisco, J.; Gutiérrez, B.; González, J. Role of the Ubiquitin-Proteasome Systems in the Biology and Virulence of Protozoan Parasites. *BioMed Res. Int.* **2015**, *2015*, 141526. [CrossRef] [PubMed]
16. Rojas, F.; Koszela, J.; Búa, J.; Llorente, B.; Burchmore, R.; Auer, M.; Mottram, J.C.; Téllez-Iñón, M.T. The Ubiquitin-Conjugating Enzyme CDC34 Is Essential for Cytokinesis in Contrast to Putative Subunits of a SCF Complex in Trypanosoma Brucei. *PLoS Negl. Trop. Dis.* **2017**, *11*, e0005626. [CrossRef]
17. Gupta, I.; Aggarwal, S.; Singh, K.; Yadav, A.; Khan, S. Ubiquitin Proteasome Pathway Proteins as Potential Drug Targets in Parasite Trypanosoma Cruzi. *Sci. Rep.* **2018**, *8*, 8399. [CrossRef]
18. Bijlmakers, M.-J. Ubiquitination and the Proteasome as Drug Targets in Trypanosomatid Diseases. *Front. Chem.* **2020**, *8*, 630888. [CrossRef]
19. Del Pino, R.C.; Zoltner, M.; Yamada, K.; Butterfield, E.R.; Field, M.C. Evolution of Cullin E3 Ubiquitin Ligases and Function in Trypanosomes. *bioRxiv* **2023**. [CrossRef]
20. Alonso, V.L.; Escalante, A.M.; Rodríguez Araya, E.; Frattini, G.; Tavernelli, L.E.; Moreno, D.M.; Furlan, R.L.E.; Serra, E. 1,3,4-Oxadiazoles as Inhibitors of the Atypical Member of the BET Family Bromodomain Factor 3 from Trypanosoma Cruzi (TcBDF3). *Front. Microbiol.* **2024**, *15*, 1465672. [CrossRef]
21. Alonso, V.L.; Ritagliati, C.; Cribb, P.; Cricco, J.A.; Serra, E.C. Overexpression of Bromodomain Factor 3 in Trypanosoma Cruzi (TcBDF3) Affects Differentiation of the Parasite and Protects It against Bromodomain Inhibitors. *FEBS J.* **2016**, *283*, 2051–2066. [CrossRef] [PubMed]
22. Sahni, J.M.; Keri, R.A. Targeting Bromodomain and Extraterminal Proteins in Breast Cancer. *Pharmacol. Res.* **2018**, *129*, 156–176. [CrossRef]
23. Wang, N.; Wu, R.; Comish, P.B.; Kang, R.; Tang, D. Pharmacological Modulation of BET Family in Sepsis. *Front. Pharmacol.* **2021**, *12*, 642294. [CrossRef] [PubMed]
24. Duan, W.; Yu, M.; Chen, J. BRD4: New Hope in the Battle against Glioblastoma. *Pharmacol. Res.* **2023**, *191*, 106767. [CrossRef]
25. Pezza, A.; Tavernelli, L.E.; Alonso, V.L.; Perdomo, V.; Gabarro, R.; Prinjha, R.; Rodríguez Araya, E.; Rioja, I.; Docampo, R.; Calderón, F.; et al. Essential Bromodomain TcBDF2 as a Drug Target against Chagas Disease. *ACS Infect. Dis.* **2022**, *8*, 1062–1074. [CrossRef]
26. Abramson, J.; Adler, J.; Dunger, J.; Evans, R.; Green, T.; Pritzel, A.; Ronneberger, O.; Willmore, L.; Ballard, A.J.; Bambrick, J.; et al. Accurate Structure Prediction of Biomolecular Interactions with AlphaFold 3. *Nature* **2024**, *630*, 493–500. [CrossRef]
27. Rodríguez Araya, E.; Serra, E. Context-Dependent Protein Structure Prediction Analysis and Stoichiometry Inference with MultimerMapper. *bioRxiv* **2025**. [CrossRef]
28. Angers, S.; Li, T.; Yi, X.; MacCoss, M.J.; Moon, R.T.; Zheng, N. Molecular Architecture and Assembly of the DDB1-CUL4A Ubiquitin Ligase Machinery. *Nature* **2006**, *443*, 590–593. [CrossRef]

29. Calabrese, M.F.; Scott, D.C.; Duda, D.M.; Grace, C.R.R.; Kurinov, I.; Kriwacki, R.W.; Schulman, B.A. A RING E3-Substrate Complex Poised for Ubiquitin-like Protein Transfer: Structural Insights into Cullin-RING Ligases. *Nat. Struct. Mol. Biol.* **2011**, *18*, 947–949. [CrossRef]
30. Chamberlain, P.P.; Lopez-Girona, A.; Miller, K.; Carmel, G.; Pagarigan, B.; Chie-Leon, B.; Rychak, E.; Corral, L.G.; Ren, Y.J.; Wang, M.; et al. Structure of the Human Cereblon-DDB1-Lenalidomide Complex Reveals Basis for Responsiveness to Thalidomide Analogs. *Nat. Struct. Mol. Biol.* **2014**, *21*, 803–809. [CrossRef]
31. Fischer, E.S.; Böhm, K.; Lydeard, J.R.; Yang, H.; Stadler, M.B.; Cavadini, S.; Nagel, J.; Serluca, F.; Acker, V.; Lingaraju, G.M.; et al. Structure of the DDB1–CRBN E3 Ubiquitin Ligase in Complex with Thalidomide. *Nature* **2014**, *512*, 49–53. [CrossRef] [PubMed]
32. Hartmann, M.D.; Boichenko, I.; Coles, M.; Lupas, A.N.; Hernandez Alvarez, B. Structural Dynamics of the Cereblon Ligand Binding Domain. *PLoS ONE* **2015**, *10*, e0128342. [CrossRef] [PubMed]
33. Esmaeili, A.; Yoosefian, M.; Mahani, M. Molecular Dynamics Simulation of Lenalidomide Interaction with cRBN Protein: A Target for Immunomodulatory Drugs. *S. Afr. J. Chem.* **2023**, *77*, 157–162. [CrossRef]
34. Hao, Q.; Rathinaswamy, M.K.; Klinge, K.L.; Bratkowski, M.; Mafi, A.; Baumgartner, C.K.; Hamel, K.M.; Veits, G.K.; Jain, R.; Catalano, C.; et al. Mechanistic Insights into a Heterobifunctional Degrader-Induced PTPN2/N1 Complex. *Commun. Chem.* **2024**, *7*, 183. [CrossRef]
35. Wu, K.Y.; Hung, T.I.; Chang, C.-E.A. PROTAC-Induced Protein Structural Dynamics in Targeted Protein Degradation. *eLife* **2025**, *13*, RP101127. [CrossRef]
36. Matyskiela, M.E.; Couto, S.; Zheng, X.; Lu, G.; Hui, J.; Stamp, K.; Drew, C.; Ren, Y.; Wang, M.; Carpenter, A.; et al. SALL4 Mediates Teratogenicity as a Thalidomide-Dependent Cereblon Substrate. *Nat. Chem. Biol.* **2018**, *14*, 981–987. [CrossRef]
37. Tao, J.; Yang, J.; Xu, G. The Interacting Domains in Cereblon Differentially Modulate the Immunomodulatory Drug-Mediated Ubiquitination and Degradation of Its Binding Partners. *Biochem. Biophys. Res. Commun.* **2018**, *507*, 443–449. [CrossRef]
38. Asatsuma-Okumura, T.; Ito, T.; Handa, H. Molecular Mechanisms of Cereblon-Based Drugs. *Pharmacol. Ther.* **2019**, *202*, 132–139. [CrossRef]
39. Min, Y.; Wi, S.M.; Kang, J.-A.; Yang, T.; Park, C.-S.; Park, S.-G.; Chung, S.; Shim, J.-H.; Chun, E.; Lee, K.-Y. Cereblon Negatively Regulates TLR4 Signaling through the Attenuation of Ubiquitination of TRAF6. *Cell Death Dis.* **2016**, *7*, e2313. [CrossRef]
40. Zhou, L.; Hao, Z.; Wang, G.; Xu, G. Cereblon Suppresses the Formation of Pathogenic Protein Aggregates in a P62-Dependent Manner. *Hum. Mol. Genet.* **2018**, *27*, 667–678. [CrossRef] [PubMed]
41. Kurihara, T.; Asahi, T.; Sawamura, N. Cereblon-Mediated Degradation of the Amyloid Precursor Protein via the Ubiquitin-Proteasome Pathway. *Biochem. Biophys. Res. Commun.* **2020**, *524*, 236–241. [CrossRef]
42. Hartmann, M.D.; Boichenko, I.; Coles, M.; Zanini, F.; Lupas, A.N.; Hernandez Alvarez, B. Thalidomide Mimics Uridine Binding to an Aromatic Cage in Cereblon. *J. Struct. Biol.* **2014**, *188*, 225–232. [CrossRef]
43. Heim, C.; Spring, A.-K.; Kirchgäßner, S.; Schwarzer, D.; Hartmann, M.D. Identification and Structural Basis of C-Terminal Cyclic Imides as Natural Degrons for Cereblon. *Biochem. Biophys. Res. Commun.* **2022**, *637*, 66–72. [CrossRef] [PubMed]
44. Ichikawa, S.; Flaxman, H.A.; Xu, W.; Vallavoju, N.; Lloyd, H.C.; Wang, B.; Shen, D.; Pratt, M.R.; Woo, C.M. The E3 Ligase Adapter Cereblon Targets the C-Terminal Cyclic Imide Degron. *Nature* **2022**, *610*, 775–782. [CrossRef] [PubMed]
45. Nakagawa, M.; Nakagawa, T. CUL4-Based Ubiquitin Ligases in Chromatin Regulation: An Evolutionary Perspective. *Cells* **2025**, *14*, 63. [CrossRef]
46. Shabek, N.; Ruble, J.; Waston, C.J.; Garbutt, K.C.; Hinds, T.R.; Li, T.; Zheng, N. Structural Insights into DDA1 Function as a Core Component of the CRL4-DDB1 Ubiquitin Ligase. *Cell Discov.* **2018**, *4*, 67. [CrossRef]
47. He, Y.J.; McCall, C.M.; Hu, J.; Zeng, Y.; Xiong, Y. DDB1 Functions as a Linker to Recruit Receptor WD40 Proteins to CUL4-ROC1 Ubiquitin Ligases. *Genes Dev.* **2006**, *20*, 2949–2954. [CrossRef]
48. Buckner, F.S.; Verlinde, C.L.; La Flamme, A.C.; Van Voorhis, W.C. Efficient Technique for Screening Drugs for Activity against Trypanosoma Cruzi Using Parasites Expressing Beta-Galactosidase. *Antimicrob. Agents Chemother.* **1996**, *40*, 2592–2597. [CrossRef]
49. Alonso, V.L.; Manarin, R.; Perdomo, V.; Gulin, E.; Serra, E.; Cribb, P. In Vitro Drug Screening Against All Life Cycle Stages of Trypanosoma Cruzi Using Parasites Expressing β-Galactosidase. *J. Vis. Exp. JoVE* **2021**, *177*, e63210. [CrossRef]
50. Tavernelli, L.E.; Alonso, V.L.; Peña, I.; Rodríguez Araya, E.; Manarin, R.; Cantizani, J.; Martin, J.; Salamanca, J.; Bamborough, P.; Calderón, F.; et al. Identification of Novel Bromodomain Inhibitors of Trypanosoma Cruzi Bromodomain Factor 2 (TcBDF2) Using a Fluorescence Polarization-Based High-Throughput Assay. *Antimicrob. Agents Chemother.* **2024**, *68*, e0024324. [CrossRef]
51. Alvarez-Jarreta, J.; Amos, B.; Aurrecoechea, C.; Bah, S.; Barba, M.; Barreto, A.; Basenko, E.Y.; Belnap, R.; Blevins, A.; Böhme, U.; et al. VEuPathDB: The Eukaryotic Pathogen, Vector and Host Bioinformatics Resource Center in 2023. *Nucleic Acids Res.* **2024**, *52*, D808–D816. [CrossRef]
52. van Kempen, M.; Kim, S.S.; Tumescheit, C.; Mirdita, M.; Lee, J.; Gilchrist, C.L.M.; Söding, J.; Steinegger, M. Fast and Accurate Protein Structure Search with Foldseek. *Nat. Biotechnol.* **2024**, *42*, 243–246. [CrossRef] [PubMed]
53. Altschul, S.F.; Madden, T.L.; Schäffer, A.A.; Zhang, J.; Zhang, Z.; Miller, W.; Lipman, D.J. Gapped BLAST and PSI-BLAST: A New Generation of Protein Database Search Programs. *Nucleic Acids Res.* **1997**, *25*, 3389–3402. [CrossRef] [PubMed]

54. Case, D.A.; Aktulga, H.M.; Belfon, K.; Cerutti, D.S.; Cisneros, G.A.; Cruzeiro, V.W.D.; Forouzesh, N.; Giese, T.J.; Götz, A.W.; Gohlke, H.; et al. AmberTools. *J. Chem. Inf. Model.* **2023**, *63*, 6183–6191. [CrossRef] [PubMed]
55. Jorgensen, W.L.; Chandrasekhar, J.; Madura, J.D.; Impey, R.W.; Klein, M.L. Comparison of Simple Potential Functions for Simulating Liquid Water. *J. Chem. Phys.* **1983**, *79*, 926–935. [CrossRef]
56. Maier, J.A.; Martinez, C.; Kasavajhala, K.; Wickstrom, L.; Hauser, K.E.; Simmerling, C. ff14SB: Improving the Accuracy of Protein Side Chain and Backbone Parameters from ff99SB. *J. Chem. Theory Comput.* **2015**, *11*, 3696–3713. [CrossRef]
57. Roe, D.R.; Cheatham, T.E. PTRAJ and CPPTRAJ: Software for Processing and Analysis of Molecular Dynamics Trajectory Data. *J. Chem. Theory Comput.* **2013**, *9*, 3084–3095. [CrossRef]
58. McGann, M. FRED and HYBRID Docking Performance on Standardized Datasets. *J. Comput. Aided Mol. Des.* **2012**, *26*, 897–906. [CrossRef]